Optical Properties of $(CdO)_x(ZnO)_{1-x}$ Thin Films Grown by Non–conventional Spray Pyrolysis

E. K. Elmaghraby [a], M. A. Kaid [b], M. F. Zaki [a], and K. Abdel-Hady [b]

[a]Experimental Nuclear Physics Department, Nuclear Research Center, Atomic Energy Authority, Cairo 13759, Egypt.
[b]Physics Department, Faculty of Science, Minia University, Egypt.

Composite cadmium oxides – zinc oxides, $(CdO)_x(ZnO)_{1-x}$, thin films are grown with variable composition, x, by non–conventional spray pyrolysis technique from two separate cavities. X-ray diffraction proves the formation of cadmium and zinc peroxides upon deposition. Further annealing in air causes a loss of crystallographic order in zinc oxide grains. Annealing does not affect the structure of cadmium peroxide. The optical constants are estimated by the Murmann's exact equation from transmittance and reflectance in the wavelength range between 400 and 2400 nm and show normal dispersion. Highest luminescent yield is assigned for samples with composition x = 0.5. Annealing causes increase in luminescence yield of $(CdO)_x(ZnO)_{1-x}$ films that could be explained in the framework of structural change.

1. Introduction:

Zinc oxides, ZnO and ZnO_2, are a wide band gap material with large exciton binding energy[1]. Plain ZnO is recognized as a promising photonic material in the blue-UV region with strong near-band edge emission peak, which is assigned as due to the recombination of free excitons [2]. ZnO [3] and CdO [4] are well known, particularly as emulsion powders. However, cadmium oxides, CdO and CdO_2, are usually employed after doping with different elements or element oxides like In_2O_3 [5], F[6], and Al [7, 8] in order to enhance its electrical conduction. Zinc oxides also may be combined with cadmium [9] for the same purpose. Doping can control the electronic and luminescence properties of the active material [10, 11], on the other hand, dilution of active material in an inactive one could make promising properties. Djurisic and Leung [12] had mentioned that the optically important broad emission around 520 nm in ZnO is typically due to the existence of surface defects. This band could be altered by modification of surface area [13, 14], doping with several metal and non-metal ions [10, 11], annealing in oxygen[15], and decreasing film electrical

conductivity [16]. Last phenomenon enhances the photoluminescence (PL) properties of ZnO, consequentially; dilution of ZnO in to a higher resistivity matrix may enhance the luminescence properties of the deposited film. On the other hand, CdO is an n-type semiconductor with a well-established direct band gap at approximately 2.5 eV and resistivity 3×10^{-3} Ω cm^{-1}[17]. Mixed oxides such as CdO – In_2O_3 [5], Li_2O–CdO–P_2O_5 [18] and CdO–ZnO [19] have recently received considerable attention, since they combine many beneficial characteristics of its components. Besides, peroxides have many applications. The photocatalytic activity of CdO_2 nanocrystals is studied by Liu et al.[20] while the negative photoconductivity in cadmium oxide–zinc oxide films was observed by Kavasoglu et al. [21].

In the present work different technique for preparation of composite $(CdO)_x(ZnO)_{1-x}$ thin film with different compositions was employed to ensure that the deposition without the formation of the dilute solution $(Cd_xZn_{1-x})O$ phases. The acronyms (CdO) and (ZnO) will be used through out this work to refer to all cadmium oxides and zinc oxides, respectively.

2. Experimental Details:

2.1. Samples Preparation:

Cadmium oxides – zinc oxides composite thin films are deposited on glass substrates by non-conventional spray pyrolysis technique (Patent No. 023360 Egyptian Patent Office [22]). As presented in Fig. (1), the technique involves production of the spray droplets in two isolated cavities followed by separate filtration of the droplets by Stock's filter associated with each cavity. After the Stock's filter, the density of droplets become very low. The droplets are carried out by filtered air to a mixer in which the streams are mixed homogeneously with small coagulation ratio. The low density of droplets in the carrying tube ensure that the coagulation rate among droplets be minimum. The technique also involves carrying the aerosols to an impactor using low-bending tube to an impactor that forces the droplets to deposit on the surface of the hot substrate in homogenous and regulated manner.

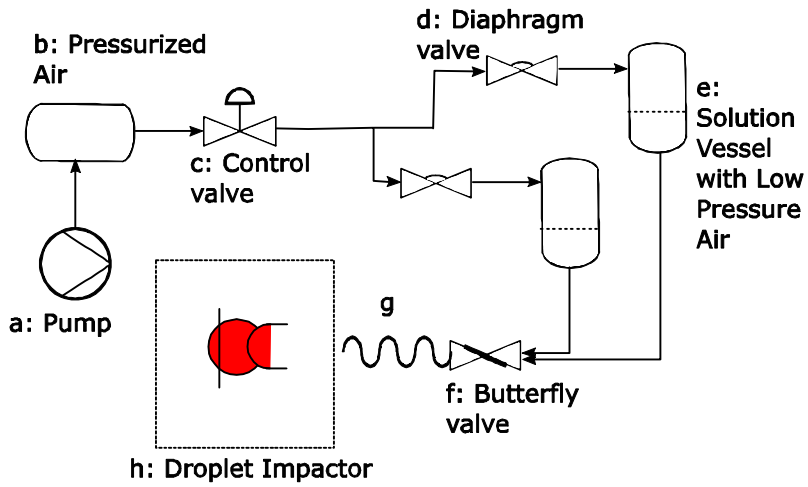

Fig, (1): Schematic diagram of the deposition setup.

The base solutions, used in the present experiment, are 0.1 ± 0.01 m aqueous solutions of zinc nitrate hexahydrate and cadmium nitrate tetrahydrate, while the deposition take place on chemically and ultrasonically cleaned glass substrates. The overall reaction process can be expressed as heat decomposition of the salt to clusters of zinc oxides and cadmium oxide in the presence of water and air oxygen. The substrate temperature during deposition was 300 ± 20 ^{o}C. Five series of samples are prepared, each with different value of composition parameter x, specifically for x = 0, 0.33, 0.5, 0.66, and 1.

After preparation, samples are subjected to successive annealing processes in air. The annealing process continued 6 h at 300 ± 5 ^{o}C followed by 6 h at 350 ± 5 ^{o}C and additional 6 h at 400 ± 5 ^{o}C. The measurements are performed before, in between and after these three processes.

2.2. Structure Measurement:

To investigate the structure of the films, a JEOL X-ray diffractometer (Model JSDX-60PA) with nickel filtered Cu:K_{α} radiation (λ = 1.5418 Å) is employed to obtain diffraction patterns. Continuous scanning is applied with a slow scanning speed and small time constant. A range of 2θ from 10^{o} to 50^{o} is scanned, so that all important diffraction peaks could be detected**.**

2.3 Optical Measurement

The optical transmittance and reflectance of the films are recorded in the wavelength range from 190 nm to 2500 nm using SHIMADZU UV 3101 PC

UV–Vis.–NIR double beam spectrophotometer. Baseline measurements are performed with two clean glass substrates situated through the spectrometer beams. The reference sample is kept to be a glass of the same type as the deposition substrates. The accuracy of the measured transmittance and reflectance is as low as 1%. Room-temperature photon induced fluorescence measurements are carried out by SHIMADZU RF-1501 double monochromator spectrometer. The 220 nm exciting wavelength of an xenon lamp is used as a result of excitation scan. The incident radiation makes an angle of 45^o to the normal axis of the sample while the luminescent radiation is detected at angle 90^o to the incident radiation. To prevent detector to reach its maximum value, the excitation opening slit is covered by a piece of dark thick paper punched with a slit of width 2 mm. For luminescence, it is difficult to reproduce the exactly same measurement due to the change in Xenon lamp temperature with operation. Only the spectra that are taken in the same run that are compared.

2.4 Thickness Measurement

The film thickness of the prepared samples are measured using multiple beam Fizeau fringes at reflection using either white light or a monochromatic light (Hg, λ_g=546 nm). The colored interference fringes enable the determination of the integer number of the fringe shift, while using the monochromatic light, fringe shift as a fraction of order separation, is measured using an eyepiece micrometer. The accuracy of this technique is less than 7%.

3 Results and Discussions

3.1 X-ray Diffraction Measurements

Diffractograms, Fig. (2), for the as-deposited samples and samples annealed at 300 ^oC and 350 ^oC show the formation of cadmium and zinc peroxides (reflections (111) of CdO_2, and (100) of ZnO_2). The monoxides phases are not observed in the as deposited sample. After annealing, the zinc peroxide peaks, (111), disappeared. After annealing, the plane (111) of CdO_2 is no observed as shown Fig (2), due to attributed to the formation of the hexagonal wurtzite structure of ZnO from the cubic structure of ZnO_2. As a result of the change in the space orientation, the crystallites suffer of a kind of disorder, which causes diminishing the diffraction pattern While the cubic structure of cadmium oxides does not change by heat annealing. Han et al. [23] proved the formation monoxide $Cd_{1-x}Zn_xO$ from the peroxide after annealing at 400 ^oC for 4 h, while in our work the situation still the same as after annealing at 350 ^oC. The our results are attributed to the existence of morphological difference between our and their samples.. Also, if the zinc peroxide deposited alone, the loss of crystal order

happens; that is obvious in work of Lindroos and Leskelä [24]. That facts supports the attribute of formation of two oxide composite system even after annealing at 400 °C. Another supporting observation, is the existence of the crystalline phase in the transformation from cubic structure of cadmium peroxide CdO_2 into CdO with a cubic structure after annealing in results of de Léon-Gutiérrez et al. [25]. In the present work, CdO_2 is still exists even after annealing at 400 °C.

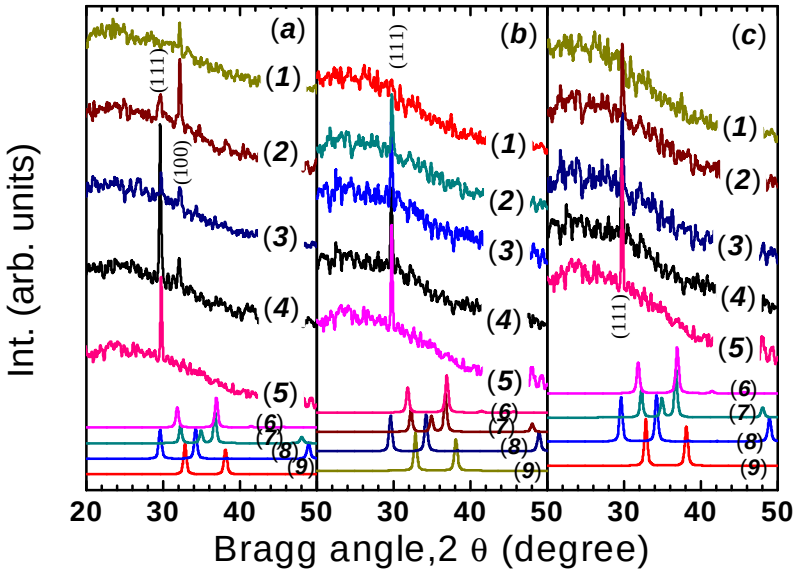

Fig. (2): XRD Diffractorgrams of samples: (a) deposited at 300 °C, (b) annealed for 6 h at 350 °C and (c) annealed for 6 h at 400 °C. Curves labeled 1–5 refer to sample with composition x = 0, 0.33, 0.5, 0.66 and 1 respectively. Labels 6 – 9 refer to calculated powder diffraction pattern for cadmium oxide, cadmium peroxide, zinc oxide, and zinc peroxide, respectively.

3.2 Transmittance and Reflectance Measurements

Figure (3) represents the transmittance and reflectance spectra of the deposited samples. The measured transmittance, $T_m(\lambda)$, is corrected by multiplying it by the measured substrate transmittance, $T_G(\lambda)$ to obtain the corrected transmittance, $T_c(\lambda)$. Hence, the product $T_m(\lambda)\times T_G(\lambda)$ represents the number of photons passed through the sample upon incidence of one photon. The prepared films show high transmittance ($T > 0.75$) and low reflectance over all the investigated range from wavelength Fig. (3).

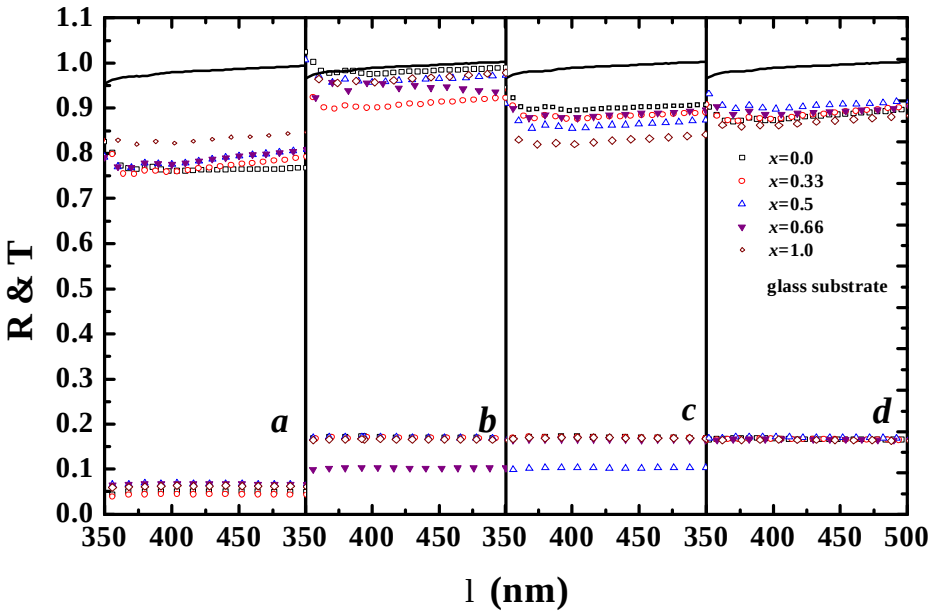

Fig. (3): Plot of the corrected transmittance and reflectance curves versus wavelength for: a) as deposited samples, b) samples annealed at 300°C, c) samples annealed at 350°C and d) samples annealed at 400°C. Curves are for different values of x and lower curves are for reflectance.

Refractive index, n, has been obtained from the corrected T and R using a previously developed computation method [28]. The technique involves bivariant search based on minimizing the difference between calculated and experimental transmittance T and reflectance R assuming an initial guess of the optical constants. Calculated T and R are given by Murmann's exact equations [29, 30]. The spectral behavior of the calculated refractive index, n, is shown in Fig.(4) for the wavelength range from 0.4 to 2.4 μm, with uncertainty 7% in thickness measurement and about 10% in the calculation. The measured film thickness range from 80 to 100 nm according to the composition, x. In the figure, the separate points represent derived values using the illustrated procedure, while continuous lines are the fitting curves using Sellmeier's relation [31–33]

$$n = n_{\infty} + \frac{b^2}{l^2 - l_o^2} \qquad (1)$$

Here, n_{∞}, b, and λ_o are constants. All films show similar behavior exhibiting normal dispersion. However, the values of refractive index are less than that given in literature which may be due to the technique of deposition of the films make it less optically dense. In Fig. (4a), the composition parameter x affects the refractive index due to the formation of two oxides with different optical

properties, namely CdO_2 and ZnO_2. For samples annealed above 350 ^oC, this effect is not remarkable and takes place within the value of uncertainty. For samples deposited and annealed at 300 ^oC, the value of n_∞ vary with x. By annealing, the refractive index increases to the range 1.65–1.67 in agrement with the trend illustrated in the work of Lindroos and Leskelä [24]. Lindroos and Leskelä showed that the refractive indices of the ZnO_2 films grown at room temperature on glass substrate increased from 1.76–1.91 to 1.98–2.07 after annealing at 200 ^oC. According to the results of structural determination, the change in refractive index could be explained to be as a result of full or partial transformation of ZnO_2 and CdO_2 to ZnO and CdO after annealing.

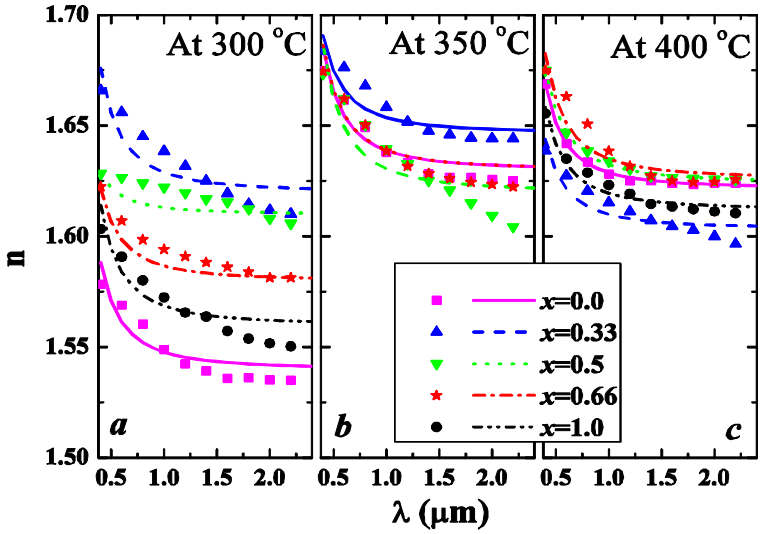

Fig. (4): The dependence of refractive index on wavelength for samples prepared with different composition and treated at a) 300^{o}C, b) 350^{o}C, and c) 400^{o}C. Separate points represent derived values while continuous lines are the fitting curves using Sellmeier's relation.

3.3 Luminescence Measurements

Due to the 45^o setup of the fluorometer, part of the photons that is coming from the excitation monochromator are reflected and counted by the emission monochromator. These reflections are room-temperature luminescence spectra are excitated by wavelength λ_{ex} = 220 nm. The as-deposited ZnO_2 films have higher luminescence yield with respect to CdO_2 films. However, any mixture of the CdO_2 with ZnO_2 gives the film an enhanced luminescence yield than the original (CdO) and (ZnO) films. The maximum luminescence yield is found to be for x = 0.5.

In contrast to our results, Mares et al. [34] give the integrated luminescent radiation that is increasingly changed with increasing the ratio of Cd in the sample. According to Mares et al. work, the material is compound $Cd_xZn_{1-x}O$ not clear a composition oxide. The increase in the interface area due to solid state dilution of (CdO) in (ZnO), and vise versa, explains the enhancement of the luminescence intensity donated at x = 0.5. The presence of conductive (ZnO) cluster embodied in higher resistance (CdO) matrix will enhance the recombination of e-h excitons in the (ZnO) clusters. On this bases the increase of luminescence yield could be attributed to the high resistivity of cadmium oxides, that has high resistivity values of 2 to 20 $\times$ 10^{-4} Ωcm^{-1} for those films deposited by different techniques such as reactive sputtering [35] and chemical vapor deposition[36], whereas for simpler techniques such as spray pyrolysis, resistivity values are reported to be between 10^{-3} and 10^{-2} Ωcm^{1} [37].

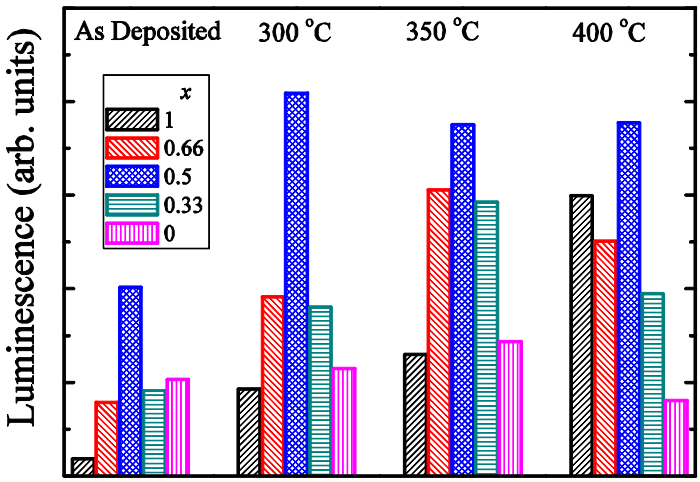

Fig. (5): The integrated luminescence yield due to the annealed samples in addition to the as deposited samples.

To enable direct comparison between the luminescence spectra measured for different samples at different annealing temperatures, the integrated luminescence yields are calculated and presented in bar plot, Fig.(5). The general trend of the (CdO)–(ZnO) films is to enhance the luminescence properties of the as deposited films by annealing at 300 °C. However, further annealing reduces the luminescence yield. Such increase in the luminescence yield by annealing does not conflict with the observation of decrease in forward luminescent radiation by annealing observed in transmittance geometry. The later arise from unavoidable usage of glass substrate during calibration of the spectrophotometer and nonlinear optical processes. .

The yield of CdO films (x = 1) increases by annealing. This can be attributed to the decrease in the resistivity of CdO (with a small preferential orientation of the (111) plane) by approximately one order of magnitude as the T_{sub} increases reaching a minimum value of 6×10^{-4} Ω cm^{-1} at 350 ^{o}C [37]. By approaching the lower resistance, e–h excitons are able to reach (within its life time) the interface among (CdO) grains and recombine radiatively, a comparable trend could describe sample with value of x =0. The yield increases for samples with x = 0.33 and 0.66 as a result of migration of excitons from CdO grains to to recombine radiatively in ZnO grains. With increasing the annealing time and temperature, the resistivity of CdO decreases which allows fast recombination of e–h pairs before reaching ZnO grains; which in turns reduces the yield.

The main feature of the excitonic recombination is the time constant. Non-radiative renominations give rise upon a fast relaxation of the excited carriers, while the slow exciton decay causes the radiative recombination of free or localized excitons [38]. It has been reported that the radiative recombination of excitons in semiconductors is in the order of ≥1 ns [39]. Additional sources of the non-radiative recombination may be caused by Auger effect and multiphonon scattering [40]. In fact, different lifetime behavior has been observed for ZnO with a fast time constant ranging from 10 to several tens of ps and a slow term ranging from several hundreds of ps to nearly 20 ns, and the reported decay time is usually smaller than 100 ps when a stimulated emission or a lasing action took place in ZnO nanocrystals [41, 42]. Recently, Wilkinson et al. [43] have reported that a free excitons in ZnO single crystal have a lifetime of 403 ps at room temperature and the lifetime of trapped carriers is approximated to 3.8 ns. In nanocrystalline ZnO thin films, Bauer et al. [44] reported that a direct radiative recombination of excitons can take place with a time constant of 12 ps. Moreover, Guo et al. [40] reported that the time constant for the capture of free excitons at the band-tail states is in the order of 30 ps, and a slower decay term of 100–400 ps is associated with radiative recombination of free or localized excitons.

4. Conclusion:

The $(CdO)_x(ZnO)_{1-x}$ thin films with variable composition, x, are grown by non–conventional spray pyrolysis technique from two separate cavities. X-ray diffraction shows the formation of cadmium and zinc peroxides upon deposition. Further annealing causes a loss of crystallographic order in zinc oxide grains. Annealing up to 400 ^{o} C causes changes in the structure of each oxide without an evidence for the formation of the mixed compound $Cd_xZn_{1-x}O$. The structural changes affect the optical properties of the films.

References

1. C. Klingshirn, phys. status solidi, B **71,** 547 (1975).
2. D. Bagnall, Y. Chen, Z. Zhu, T. Yao, S. Koyama, M. Shen, T. Goto, *Appl. Phys. Lett*. **70**, 2230 (1997).
3. P. Kamat, B. Patrick, *J. Phys. Chem*. **96**, 6829 (1992).
4. D. Tryk, A. Fujishima, K. Honda, *Electrochim. Acta*, **45**, 2363 (2000).
5. [5] H. Ali, H. Mohamed, M. Wakkad, M. Hasaneen, *Thin Solid Films*, **515**, 3024 (2007).
6. J. Chen, J.Wang, F. Zhang, G. Zhang, Z. G. Wu, P. Yana, *J. Cryst. Growth*, **310**, 2627 (2008).
7. R. Maity, K. Chattopadhyay, *Solar Energy Mater. Solar Cells*, **90**, 597 (2006).
8. B. Saha, S. Das, K. Chattopadhyay, *Solar Energy Mater. Solar Cells*, **91** (18), 1692 (2007).
9. U. N. Maiti, P. K. Ghosh, S. F. Ahmed, M. K. Mitra, K. K. Chattopadhyay, *J. Sol-Gel Sci. Techn*., **41**, 87 (2007).
10. Y. Wang, P. Thomas, P. OBrien, *J. Phys. Chem*., **B 110** (43), 21412 (2006).
11. S. Singh, N. Rama, M. S. R. Rao, *Appl. Phys. Lett*., **88** (22), 222111 (2006).
12. A. Djurisic, Y. Leung, Small, **2** (8–9), 944 (2006).
13. van Dijken, J. Makkinje, A. Meijerink, *J. Luminescence*, **92** (4), 323 (2001).
14. van Dijken, E. Meulenkamp, D. Vanmaekelbergh, A. Meijerink, *J. Phys. Chem*., **B 104**, 1715 (2000).
15. K. Vanheusden, W. Warren, C. Seager, D. Tallant, J. Voigt, B. Gnade, *J. Appl. Phys*., **79**, 78983 (1996).
16. K. Ramamoorthy, C. Sanjeeviraja, M. Jayachandran, K. Sankaranarayanan, P. Misra, L. Kukreja, *Curr. App. Phys*., **6** (1), 103 (2005).
17. Y. Choi, C. Lee, S. Cho, *Thin Solid Films*, **289**, 153 (1996).
18. M. Altaf, M. Chaudhry, S. Siddiqi, *Mater. Chem. Phys*. **71**, 28 (2001).
19. F. Cruz-Gandarilla, A. Morales-Acevedo, O. Vigil, M. Hesiquio-Garduno, L. Vaillant, G. Contreras-Puente, *Mater. Chem. Phys*., **78**, 840 (2003).

20. Y. Liu, Y. C. Zhang, X. F. Xu, *J. Hazardous Mater*., **163**, 1310 (2009).
21. N. Kavasoglu, A. S. Kavasoglu, S. Oktik, *J. Phys. Chem. Solids*, **70**, 521 (2009).
22. E. K. Elmaghraby, "A device and method for deposition of chemical vapor and spray droplets by electrically enhanced aerodynamic control in the flow of the carrier gas", Patent 023360, *Egyptian Patent Office, Egypt* (2002).
23. X. Han, R. Liu, Z. Xu, *Thin Solid Films*, **517**, 5653 (2009).
24. S. Lindroos, M. Leskelä, Int. *J. Inorg. Mater*., **2**, 197 (2000).
25. L. de Léon-Gutiérrez, J. Cayente-Romero, J. Peza-Tapia, E. Barrera-Calva, J. Martínez-Flores, M. Ortega-López, *Mater. Lett*., **60**, 3866 (2006).
26. H. Tabet-Derraz, N. Benramdane, D. Nacer, A. Bouzidi, M. Medles, *Sol. Energy Mater. Sol. Cells*, **73**, 249 (2002).
27. K. ichi Kawamura, K. Maekawa, H. Yanagi, M. Hirano, H. Hosono, *Thin Solid Films*, **445**, 182 (2003).
28. N. El-Kadry, A. Ashour, M. F. Ahmed, K. Abdel-Hady, *Thin Solid Films*, **259**, 194 (1995).
29. O. Heavens, "*Optical Properties of Thin Films*", Dover, New York, (1965).
30. O. Heavens, "*Thin Film Physics*", Methuen, London, (1970).
31. P. Washington, H. Ong, J. Dai, R. Chang, *Appl. Phys. Lett*., **72**, 3261 (1998).
32. R. Dahmani, L. Salamanca-Riba, N. Nguyen, D. Chandler-Horowitz, B. Jonker, *J. Appl. Phys*., **76**, 514 (1994).
33. H. Kamal, E. Elmaghraby, S. Ali, K. Abdel-Hady, *J. Cryst. Growth*, **262**, 424 (2004).
34. J. Mares, F. Ruhge, A. Thompson, P. Kik, A. Osinsky, B. Hertog, A. Dabiran, P. Chow, W. Schoenfeld, *Optical Materials*, **30**, 364 (2007) .
35. L. Stolt, J. Hedstrom, M. Ruckh, J. Kessier, K. Velthaus, H. Schock, *Appl. Phys. Lett*., **62**, 597 (1993).
36. L. Dai, H. Deng, G. Chen, J. Chen, *Appl. Surface Sci*., **254** (6), 1500 (2008).
37. J. Santos-Cruz, G. Torres-Delgado, R. Castanedo-Perez, S. Jime´nez-Sandoval, O. Jime´nez-Sandoval, C.I. Zu´n˜iga-Romero, J.

Ma´rquez Marı´n, O. Zelaya-Angel, *Thin Solid Films*, **493**, 83 (2005).

38. Li, L. Guo, Z. Wu, L. Ren, X. Ai, J. Zhang, Y. Lv, H. Xu, D. Yu, *Solid State Commun*., **139**, 355 (2006).

39. A. Othonos, *J. Appl. Phys*., **83**, 1789 (1998). A

40. B. Guo, Z. Ye, K. Wong, *J. Cryst. Growth*, **253**, 252 (2003).

41. C. Soukoulis, X. Jiang, J. Xu, H. Cao, *Phys. Rev*., **B 65**, 041103 (2002).

42. M. Huang, S. Mao, H. Feick, H. Yan, Y. Wu, H. Kind, E. Weber, R. Russo, P. Yang, *Science*, **292**, 1897 (2001).

43. J. Wilkinson, K. Ucer, R. Williams, *Rad. Meas*., **38**, 501 (2004).

44. Bauer, G. Boschloo, E. Mukhtar, A. Hagfeldt, *Chem. Phys. Lett*., **387**, 176 (2004).